Characterizing subcutaneous cortical auditory evoked potentials in mice

Olivier Postal, Warren Bakay, Typhaine Dupont, Alexa Buck, Christine Petit, Nicolas Michalski, Boris Gourévitch

Hearing Research 422 (2022) 108566

Contents lists available at ScienceDirect

Hearing Research

journal homepage: www.elsevier.com/locate/heares

Short communication

Characterizing subcutaneous cortical auditory evoked potentials in mice

Olivier Postal[a,c,#], Warren Bakay[a,#], Typhaine Dupont[a], Alexa Buck[a], Élodie Daoud[a], Christine Petit[a], Nicolas Michalski[a,#], Boris Gourévitch[a,b,#,*]

[a] Institut de l'Audition, Institut Pasteur, INSERM, Université Paris Cité, F-75012 Paris, France
[b] CNRS, France
[c] Sorbonne Université, Collège Doctoral, F-75005 Paris, France

ARTICLE INFO

Article history:
Received 17 March 2022
Revised 17 June 2022
Accepted 30 June 2022
Available online 3 July 2022

Keywords:
Auditory brainstem response
Cortical auditory evoked potential

ABSTRACT

Auditory Brainstem Responses (ABRs) are a reliably robust measure of auditory thresholds in the mammalian hearing system and can be used to determine deficits in the auditory periphery. However, because these measures are limited to the lower stages of the auditory pathway, they are insensitive to changes or deficits that occur in the thalamic and cortical regions. Cortical Auditory Evoked Potentials (CAEPs), as longer latency responses, capture information from these regions. However they are less frequently used as a diagnostic tool, particularly in rodent models, due to their inherent variability and subsequent difficult interpretation.

The purpose of this study was to develop a consistent measure of subcutaneous CAEPs to auditory stimuli in mice and to determine their origin. To this end, we investigated the effect on the CAEPs recorded in response to different stimuli (noise, click, and tone (16 kHz) bursts), stimulus presentation rates (2/s, 6/s, 10/s) and electrode placements. Recordings were examined for robust CAEP components to determine the optimal experimental paradigm. We argue that CAEPs can measure robust and replicable cortical responses. Furthermore, by deactivating the auditory cortex with lidocaine we demonstrated that the contralateral cortex is the main contributor to the CAEP. Thus CAEP measurements could prove to be of value diagnostically in future for deficits in higher auditory areas.

Introduction

Auditory Brainstem Responses (ABRs) recorded near the ears are frequently used to measure auditory thresholds in mammals and can be used to identify peripheral hearing deficits. ABRs occur within the first 10 ms after sound presentation and are thought to emanate from successive activation of the ascending auditory pathway (Felix et al., 2018; Winkler et al., 2013). However, ABRs do not capture cortical activity. To circumvent this limitation, human studies have long made use of scalp electroencephalography (EEG) to focus on higher order auditory areas. In particular, click stimulation induces two main middle-latency waves in the EEG, Na/Pa (~15–35 ms) and Nb/Pb (35–60 ms) the origins of which remain controversial with most likely generators being the auditory thalamus and primary auditory cortex, while the midbrain or secondary auditory cortex are less likely (Musiek and Nagle, 2018; Picton et al., 1974). So called longer latency waves N1/P2/N2 occur at around 100/180/300 ms, respectively, and are thought to reflect higher order processing involving primary, secondary and associative auditory cortices (Godey et al., 2001; Tremblay and Burkard, 2012). These Cortical Auditory Evoked Potentials (CAEPs) have already been widely used in human studies to assess pharmacodynamics, cortical lesions, sensory processing and deficits and clinical outcomes on auditory cortical function (Davies et al., 2010; Ibañez et al., 1989; Johnson, 2009; Litscher, 1995; Supp et al., 2018; Winkler et al., 2013).

In mice, an important genetic animal model, there have been only a few studies using middle or long latency CAEPs and the majority of these were obtained epidurally (Farley et al., 2019; Metzger et al., 2007; O'Reilly and Conway, 2021; Siegel et al., 2003). Subcutaneous CAEPs are surprisingly infrequently used diagnostically despite being less invasive and still providing relatively good spatial information.

To assess the usability of subcutaneous CAEP recordings in mice, and to determine which stimulation and recording parameters produce the most robust results, we recorded CAEPs using

* Corresponding author at: 63 rue de Charenton, 75012 Paris
E-mail address: boris@pi314.net (B. Gourévitch).
# The authors contributed equally.

https://doi.org/10.1016/j.heares.2022.108566
0378-5955/

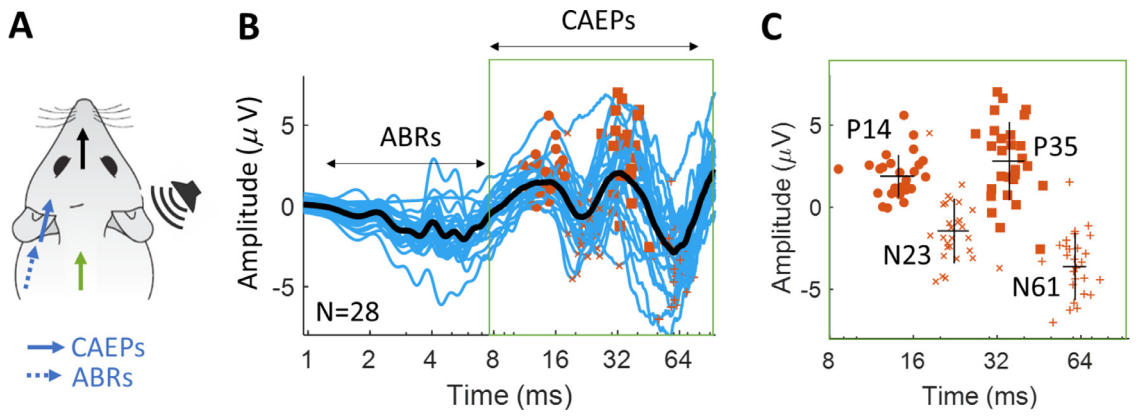

Fig. 1. *Cortical Auditory Evoked Potentials (CAEPs) in response to 5 ms noise bursts A) Electrode placements for CAEP recordings using the terminology of ABRs (IMPReSS, 2022): reference electrode (plain blue) above contralateral cortex, recording electrode (black) in rostral midline, ground (green) on the dorsum. B) Average (black) and individual (blue) CAEP traces plotted on a log timescale up to 100 ms. Orange dots indicate positive and negative maxima identified in individual curves. C) Positive and negative maxima from B (orange markers) shown without curves. The average latency for each subsequent maxima are labeled P14, N23, P35 and N61 respectively. Black crosses indicate mean and standard deviation bars in both the latency (horizontal) and amplitude (vertical) directions.*

multiple stimulus types, presentation rates and electrode placements. We also investigated their generators using auditory cortical deactivation. Our findings suggest that CAEPs in the latency range of 14–80 ms provide robust, reliable and minimally invasive measures of the contralateral thalamo-cortical response, allowing for assessment of the cortical auditory function in mice under different conditions.

Methodology

In an acoustically and electromagnetically isolated chamber, sounds were presented by Tucker-Davis Technologies (TDT) RZ6 to either closed field in-ear (TDT EC1) or free-field (TDT ES1) transducers. Electrophysiological responses were recorded from subcutaneous electrodes (SC25, NeuroService) at a 24 kHz sampling rate (TDT RA4), subjected to a Butterworth filter between 3 Hz and 3 kHz and displayed by TDT Biosigz software.

We used 90 mice (age P28–81) from strains C57BL6/JRj (56 males, 11 females), CBA/JRj (4 males, 4 females) and FVB/NRj (15 females; $n = 5$ at 112–115 days old). For all mice, ABRs/CAEPs were performed under Ketamine (150 mg/kg, Imalgene®) and Xylazine (6 mg/kg, Rompun®) anesthesia or isoflurane inhalation (between 0.6% and 1,5% isoflurane in a 95% oxygen mixture with a flow rate of 0.2 to 0.4 L/min). Hearing thresholds were measured using standard ABRs with 5 ms tone pip stimuli (2,4,8,16,24,32,48,64 kHz). Mice with thresholds more than 10 dB above normal responses (Zhang et al., 2013) were excluded and strains had comparable thresholds (Supp. Fig. 1). After ABR recordings, the post-auricular reference electrode was moved above the contralateral auditory cortex to record CAEPs (Fig. 1A).

For cortical surface evoked potential recordings, an induction cocktail (Buprenorphine 0.1 mg/kg, Ketamine 190 mg/kg, Xylazine 4.5 mg/kg) was used and mice were maintained under isoflurane inhalation. A circular craniotomy with a maximum diameter of 2 mm was performed above the auditory cortex using a tungsten carbide bur of 0.5 mm (Edenta). The craniotomy was performed contralateral to the sound presentation and centered at 2.5 mm posterior to and 4.5 mm lateral to bregma. The bone above the craniotomy window was gently detached from the dura using saline at 37 °C and removed using Dumont#5 forceps. The reference electrode was then placed next to the craniotomy subcutaneously or epidurally within the craniotomy window.

CAEP stimuli were white noise bursts or 16 kHz pure tone pips (5 ms long, 1 ms of rising and falling ramps) or 100 μs clicks, presented 100 times at a stimulus rate of 2 Hz. Statistical analyses included repeated ANOVA (RANOVA) and Wilcoxon (W) or Mann-Whitney (MW) non-parametric tests. Alpha risk is 5%.

Results

Subcutaneous recordings of CAEPs

In response to 5-ms long noise bursts, the signals recorded from electrodes over the contralateral cortex (Fig. 1A) show early subcortical peaks, typically seen in ABRs, before 8 ms and two subsequent sequences of large positive (P) and negative (N) maxima (P14, N23, P35, N61, Fig. 1BC). The reproducibility of these waves at specific latencies ensures that peaks and troughs can be identified unambiguously in each animal (Fig. 1C).

Best parameters for subcutaneous CAEP recordings

To optimize reliable and repeatable CAEP waves, we first examined the choice of stimulus (Fig. 2A). Tone stimuli produced smaller P35-N23 (peak-to-trough amplitude difference) than 5 ms noise bursts and smaller N61-P35 than both noise bursts and clicks (*N23-P14* :RANOVA, $F(2,18) = 2.72$, $p = 0.093$; *P35-N23*: RANOVA, $F(2,18) = 4.5$, $p = 0.026$, noise vs tone, $WX = 48$, $p = 0.037$; *N61-P35*: RANOVA, $F(2,18) = 4.83$, $p = 0.02$, noise vs tone, $WX = 50$, $p = 0.02$, click vs tone, $WX = 51$, $p = 0.014$). Both clicks and 5 ms noise stimuli produced similar peak-to-trough amplitudes. We thus continued our investigation using only 5 ms noise bursts.

We found similar shapes for CAEPs in males and females (Fig. 2B) but the first deflection N23-P14 had a significantly higher amplitude in males (*N23-P14*: $MW = 639$, $p = 0.014$; *P35-N23*: $MW = 582$, $p = 0.5$; *N61-P35*: $MW = 616$, $p = 0.08$). Although isoflurane led to a decrease in CAEP amplitude in some animals, compared to Ketamine/Xylazine, this effect was, on average, not significant (Fig. 2Ci&ii, *N23-P14*: $WX = 46$, $p = 0.28$; *P35-N23*: $WX = 42$, $p = 0.46$; *N61-P35*: $WX = 29$, $p = 0.76$). In addition, the type of anesthesia had no effect on latencies (*N23-P14*: $WX = 32$, $p = 0.97$; *P35-N23*: $WX = 26$, $p = 0.58$; *N61-P35*: $WX = 33$, $p = 0.92$).

We then examined the sensitivity of CAEPs to the reference electrode position (Fig. 2D). Placing the electrode at the vertex or ipsilateral cortex led to a smaller CAEP amplitude than seen with electrode above contralateral cortex especially for early waves (*N23-P14*, RANOVA, $F(3,27) = 3.5$, $p = 0.03$, contra vs vertex,

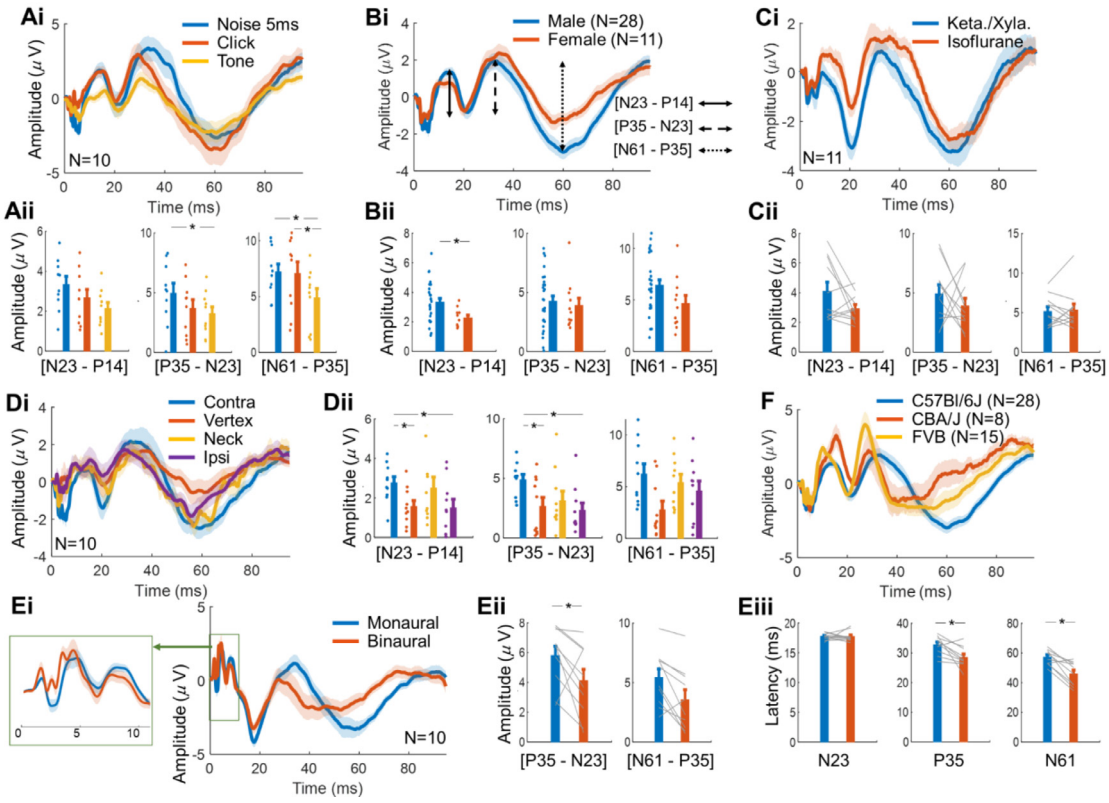

Fig. 2. Best Parameters for CAEP recordings. A) Influence of the stimulus: average CAEPs (Ai) and peak-to-trough amplitude quantification (Aii) when using a short noise burst of 5 ms (blue), a click (red) or a 16 kHz tone (yellow) as a stimulus. In Ai, pale colors around the average are standard errors. B) Same as A with the influence of sex on CAEPs. Black arrows illustrate peak-to-trough quantification in A, B, C. C) Same as A) with the influence of the anesthetic used on CAEPs. D) Same as A) with the influence of the reference electrode placement: above the contralateral auditory cortex (blue), at the vertex (red), at the neck (yellow) or above the ipsilateral auditory cortex (purple). Ei) Average CAEPs when using an insert speaker (blue, monaural, closed field) or a free field speaker at 2 cm from the ear (red). Eii) peak-to-trough amplitude quantification. Eiii) peak latency. F) Average CAEPs for three mouse strains.

$W = 53$, $p = 6e\text{-}3$; contra vs ipsi, $W = 49$, $p = 0.03$; *P35-N23*, RANOVA, $F(3,27) = 5.29$, $p = 5e\text{-}3$, contra vs vertex, $W = 48$, $p = 0.04$; contra vs ipsi, $W = 51$, $p = 0.01$; *N61-P35*, RANOVA, $F(3,27) = 2.4$, $p = 0.09$). Despite neck and contralateral cortical placements not being statistically distinguishable (*P35-N23*, WX test, $W = 44$, $p = 0.1$, *N23-P14*, WX test, $W = 36$, $p = 0.43$), less noisy CAEPs were obtained when the reference electrode was placed above the contralateral auditory cortex.

We then compared the effect of binaural and monaural stimulation, using a free field (bilateral) and close-field (unilateral) speaker, respectively. In the [0 10]ms time interval (Fig. 2E, green rectangle), peaks corresponding to classical ABRs appeared more clearly for the binaural stimulation, as the contralateral CAEP electrode acts as an ABR-like electrode for the contralateral ear stimulated by the free-field speaker. Long-latency CAEPs were modified by the binaural condition (Fig. 2E): amplitude was reduced for N61-P35 deflection (*P35-N23*: WX = 46, $p = 0.06$; *N61-P35*: WX = 50, $p = 0.02$) and latencies were shorter for P35 and N61 maxima (*N23*: WX = 37, $p = 0.36$; *P35*: WX = 52, $p = 0.01$; *N61*: WX = 54, $p = 4e\text{-}3$).

Finally, we tested the robustness of CAEP shapes in two additional mouse strains (Fig. 2F) with comparable thresholds (supp. Fig 1). We observed consistent sequences of two waves between 14 and 80 ms in all strains although peak-to-trough amplitudes and late peak latencies differed slightly from our reference C57BL6 strain.

Isolating the CAEP generators

In the following, the standard recording configuration in male C57BL6 mice was monaural stimulation with 5 ms noise bursts and recording electrode placed above contralateral auditory cortex.

To investigate the contribution of the contralateral auditory cortex to CAEPs, we adopted two strategies. First, we increased the stimulation rate because this mostly affects cortical responses. Indeed, average phase-locking abilities of neural populations decrease as one ascends the auditory system, possibly due to progressive changes in cellular and network properties (Joris et al., 2004; Rosburg and Mager, 2021). Consistently, the epidural CAEPs, which primarily reflect the auditory cortical response, showed a smaller negative peak around 25 ms with increased stimulation rate, while subsequent peaks disappeared altogether (Fig. 3A). We obtained a similar result with subcutaneous CAEPs where the amplitude and latency of peak P14 were maintained, consistent with thalamocortical activity, while the latency of N23 increased, consistent with responses of the primary auditory cortex to 10 Hz. Later peaks, with contributions from associative areas, were heavily degraded or absent (Fig. 3B).

Second, we inactivated the contralateral auditory cortex during CAEP recording using lidocaine dropped directly onto the exposed cortical surface using a pipette (Fig. 3C). After verifying that lidocaine (2–5μL, 16 mg/mL, 37 °C) reliably inactivated the contralateral auditory cortex during epidural recordings (Supp. Fig.

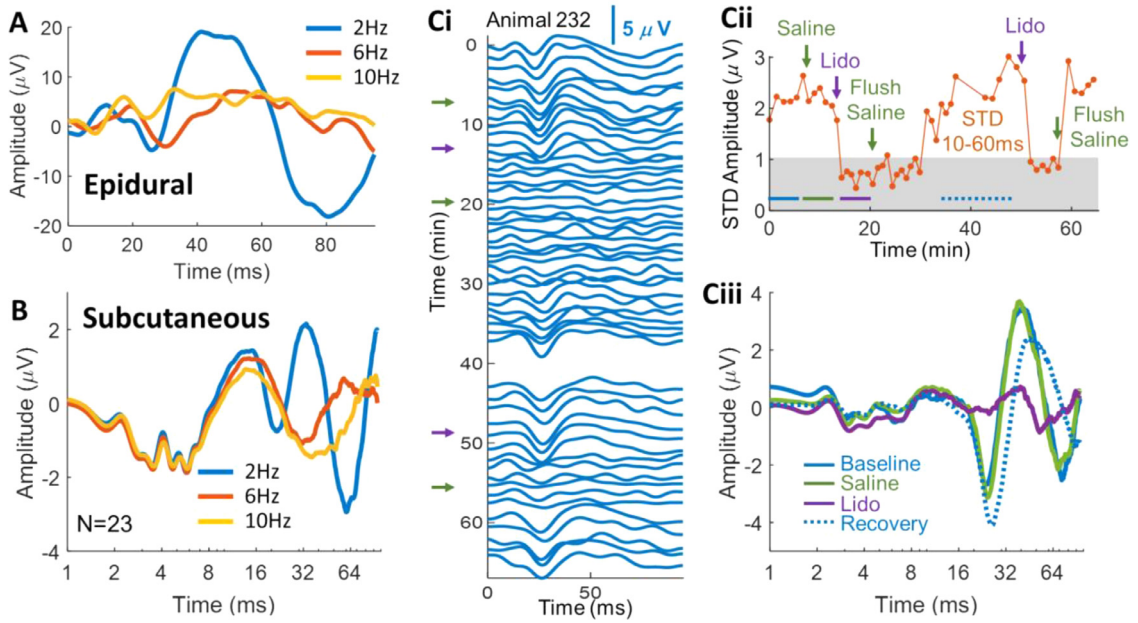

Fig. 3. Isolating the CAEP generators. A) Epidural recordings of CAEPs in one animal in response to noise bursts presented at rates of 2, 6 and 10 Hz. B) Averaged subcutaneous CAEPs for the same stimulation rates as in A. Ci) CAEPs recorded over one hour during successive application of saline (green arrows) and lidocaine (purple arrows). Instantaneous CAEPs are plotted for each time point along the y axis from stimulus onset at 0 min. Cii) Standard deviations (STD) for each trace in Ci calculated over the [8 100]ms time interval post-stimulus onset. Applications of saline and lidocaine (lido) are indicated. Gray area shows 95th percentile of STDs across CAEPs of the one-hour session, estimated on time interval [80–100]ms of each CAEP. Ciii) Averaged CAEPs before (plain blue) and after (plain green) saline application, after lidocaine (plain purple) and after saline flush (dotted blue). Corresponding times considered for averaging CAEPs are shown in Cii as horizontal plain and dotted colored bars.

2Ai,Bi), we applied the same protocol while recording subcutaneous CAEPs. Under lidocaine application, CAEPs remained unchanged until 20 ms after the stimulus onset and then flattened dramatically (Fig. 3Ciii). In addition, *contralateral* auditory cortical deactivation was sufficient to abolish most of the CAEP signal (Fig. 3Cii, replications in Supp. Fig. 3). These observations for monaural stimulation were reversible upon flushing the cortex with saline (37 °C, 300μL, 0.9%), reproducible with successive deactivation and flushing, and were similar in the case of binaural stimulation (Supp. Fig. 2 Ci). Note that prolonged CAEP latencies could be observed after recovery (Fig. 3Ciii), likely due to residual lidocaine. This effect on CAEPs has already been observed following intravenous lidocaine injections (Murofushi et al., 1994).

Discussion

Reliability of CAEP recordings

We found that CAEPs in response to noise bursts were robust. This reproducibility in amplitude and latency allows unambiguous identification of peaks and troughs across animals within [10–80]ms, latencies relevant to higher order processing (Fig. 1C). The pattern of four peaks P14, N23, P35 and N61 is maintained across all tested mouse strains (Fig. 2F) though latency and amplitude can vary between strains, corroborating previous observations in mouse epidural recordings (Siegel et al., 2003). To our knowledge, only one preprint recorded click-evoked subcutaneous CAEPs in mutant mouse models and found similar peak patterns to ours (Zinnamon et al., 2019).

Clicks are well suited to peripheral activation, such as those recorded by ABRs, insofar as they induce larger wave amplitudes than tones (Scimemi et al., 2014). In fact, both clicks and 5 ms noise bursts were able to induce larger peak-to-trough amplitudes than tones in CAEPs (Fig. 2Ai). We subsequently chose 5 ms noise bursts as they were easier to calibrate acoustically and produced a more sustained peak at the ≈35 ms latency than clicks.

As with ABRs, CAEPs in animal models are typically obtained under anesthesia, which can impact auditory processing e.g. by disrupting top-down pathways (Raz et al., 2014) and neural oscillations (Madler et al., 1991), increasing latencies (Manninen et al., 1985) and depressing cortical responses (Gaese and Ostwald, 2001; Huetz et al., 2009; Noda and Takahashi, 2015). Anesthesia typically impacts central processes more than peripheral ones (Heinke and Koelsch, 2005), and consequently CAEPs more than ABRs. Thus, it would be of interest to perform these recordings in awake animals, which has various hurdles: subcutaneous needles may cause discomfort or stress to the animal and therefore have ethical implications and induce movement artifacts in recordings. A possibility would be to wake the animal after electrode implantation under brief gas anesthesia, that latter having few persistent effects on the brain (Hambrecht-Wiedbusch et al., 2019). In our study, despite their different pharmacodynamics, we found that isoflurane and Ketamine/Xylazine elicited similar CAEP peak latencies and amplitudes. However, under isoflurane N23-P14 amplitudes were reduced, although not significantly, in many animals and signal-to-noise ratios were worse than under Ketamine/Xylazine, consistent with previous reports on ABRs (Cederholm et al., 2012; Ruebhausen et al., 2012).

Monaural and binaural stimulations provided slightly different CAEP patterns. In ABRs, a binaural component occurs as early as 3 ms in mice, possibly triggered by the activation of the superior olivary complex (Laumen et al., 2016). However, the binaural component is proportionally smaller in ABRs than in higher order auditory evoked potentials (10–300 ms), at least in humans (McPherson and Starr, 1993). Consistently, we found the biggest difference between monaural and binaural CAEPs occurred after 25–30 ms with a lower amplitude for binaural stimulation. This latter result is consistent with studies in rats and guinea-pigs (Di and Barth, 1993; Özdamar et al., 1986), which are at odds with those in cats and humans pointing towards species specific inhibitory effects following ipsilateral stimulation.

While epidural recordings used in most previous work on middle- and long-latency waves in rodents indeed show a better signal-to-noise ratio (McGee et al., 1983; Metzger et al., 2007; Siegel et al., 2003; Simpson and Knight, 1993) than CAEPs (compare the voltage levels between Fig. 3A and B), CAEPs have the clear advantage of being non-invasive. Overall, our results demonstrate CAEPs to be a robust measure of cortical activity recordable in large cohorts of animals as an adjunct to ABRs.

Generators of CAEPs

Peaks of auditory evoked potentials from short to long latencies in humans are thought to stem from spatially distinct neural generators and thus in theory can be disambiguated (Godey et al., 2001; Woods et al., 1987). Nevertheless, subcutaneous CAEP generators in mice are currently unknown.

We can attempt to identify analogous waveforms in human studies of auditory evoked potentials (Godey et al., 2001; Musiek and Nagle, 2018; Picton et al., 1974; Tremblay and Burkard, 2012). Owing to their small head size, waves in rodents should occur at shorter latencies than in humans, possibly divided by a factor of two for long latency waves (Knight et al., 1985; Siegel et al., 2003; Simpson and Knight, 1993). Thus, the complex P14/N23 in mice could correspond to the human middle latency evoked potentials and N61 would correspond to a long-latency wave as defined for humans. It remains controversial as to whether the mouse P35 is analogous to the human P50 (Simosky et al., 2003) or N100 (Siegel et al., 2003). Following in this vein, the CAEP generators would likely be in the thalamo-cortical complex, with possible contributions from non-primary auditory areas for P35 and N61.

Consistently, latencies around 14 ms are compatible with thalamus-related evoked activities (Land et al., 2016) while deep (Metzger et al., 2007; Siegel et al., 2003) and epidural (Fig. 3A) recordings show peaks at around 20 ms in the primary auditory cortex of mice. Additionally, it is known that the auditory thalamus is able to reliably respond to each noise burst at a stimulation rate around 10 Hz while the primary auditory cortical responses at this rate are reduced and even more so for higher cortical areas (Joris et al., 2004). In our study, the presentation rates above 6 Hz, and possibly above 2 Hz, preserved the early ABR and P14 peaks, but caused a delay in N23 and a collapse of the later P35 and N61 peaks suggesting these waves correspond to cortical activity.

Finally, to determine its contribution to CAEPs the auditory cortex (both primary and non-primary areas, these areas being inseparable anatomically) was inhibited using lidocaine which resulted in loss of N23, P35 and N61 peaks. Lidocaine applied to the cortical surface has been shown to not extend to the thalamus (Yang et al., 2013), the auditory region of which is particularly deep at ~3 mm below the brain surface. Therefore, it is likely that the remaining P14 arises subcortically and most likely from the auditory thalamus.

Together, this evidence would suggest a thalamic origin for P14, and an auditory cortical origin, most likely primary, for N23 and P35, compatible with middle-latency evoked potentials and consistent with previous findings on epidural recordings in mice (Siegel et al., 2003). The generators for N61 are less clear but are thought to reside in primary and non-primary auditory areas, based on its higher sensitivity to stimulus presentation rate and its latency compatible with human N1 and P2 (Siegel et al., 2003).

CRediT author statement

Olivier Postal: Investigation, Data Curation, Formal analysis, Writing; **Warren Bakay** : Investigation, Data Curation, Formal analysis, Writing, Methodology ; **Typhaine Dupont** : Investigation, Data Curation ; **Alexa Buck** : Investigation, Writing; **Élodie Daoud**: Investigation, Data Curation, Formal analysis, Methodology; **Christine Petit**: Resources, Funding acquisition; **Nicolas Michalski** : Resources, Funding acquisition, Writing – Review & Editing, Supervision; **Boris Gourévitch** : Conceptualization, Methodology, Software, Formal analysis, Writing, Visualization, Supervision.

Acknowledgements

The authors wish to thank the Animalerie Centrale of the Institut Pasteur for assistance with the project.

Data Availability

The datasets generated for this study are available on request to the corresponding author.

Ethics Statement

Animal experiments were performed in accordance with French and European regulations for the care and protection of laboratory animals (EC Directive 2010/63, French Law 2013–118), with authorization from the Institut Pasteur Ethics Committee for animal experimentation.

Funding

BG was supported by grants from the ANR (French National Research Agency, ANR-15-CE37–0007–01; ANR-21-CE34–0012). OP was supported by the Fondation pour la Recherche Médicale (FDM201806005994). AB was supported by a FET Open European Grant (Hearlight, 964568). NM was supported by grants from the ANR as part of the second Investissements d'Avenir program LIGHT4DEAF (ANR-15-RHUS-0001) and LabEx LIFESENSES (ANR-10-LABX-65), LHW-376 Stiftung, and by the Fondation pour l'Audition (FPA-IDA03).

Supplementary materials

Supplementary material associated with this article can be found, in the online version, at doi:10.1016/j.heares.2022.108566.

References

Cederholm, J.M.E., Froud, K.E., Wong, A.C.Y., Ko, M., Ryan, A.F., Housley, G.D., 2012. Differential actions of isoflurane and ketamine-based anaesthetics on cochlear function in the mouse. Hear. Res. 292, 71–79. doi:10.1016/j.heares.2012.08.010.

Davies, P., Chang, W.-P., Gavin, W., 2010. Middle and late latency ERP components discriminate between adults, typical children, and children with sensory processing disorders. Front. Integr. Neurosci. 4.

Di, S., Barth, D.S., 1993. Binaural vs. monaural auditory evoked potentials in rat neocortex. Brain Res. 630, 303–314. doi:10.1016/0006-8993(93)90670-I.

Farley, B.J., Morozova, E., Dion, J., Wang, B., Harvey, B.D., Gianni, D., Wipke, B., Cadavid, D., Wittmann, M., Hajos, M., 2019. Evoked potentials as a translatable biomarker to track functional remyelination. Molecular and Cellular Neurosci. 99, 103393. doi:10.1016/j.mcn.2019.103393.

Felix, R.A., Gourévitch, B., Portfors, C.V., 2018. Subcortical pathways: towards a better understanding of auditory disorders. Hear. Res. doi:10.1016/j.heares.2018.01.008.

Gaese, B.H., Ostwald, J., 2001. Anesthesia changes frequency tuning of neurons in the rat primary auditory cortex. J. Neurophysiol. 86, 1062–1066.

Godey, B., Schwartz, D., de Graaf, J.B., Chauvel, P., Liegeois-Chauvel, C., 2001. Neuromagnetic source localization of auditory evoked fields and intracerebral evoked potentials: a comparison of data in the same patients. Clin. Neurophysiol. 112, 1850–1859.

Hambrecht-Wiedbusch, V.S., LaTendresse, K.A., Avidan, M.S., Nelson, A.G., Phyle, M., Ajluni, R.E., Mashour, G.A., 2019. General anesthesia does not have persistent effects on attention in rodents. Front. Behav. Neurosci. 13, 76. doi:10.3389/fnbeh.2019.00076.

Heinke, W., Koelsch, S., 2005. The effects of anesthetics on brain activity and cognitive function. Curr. Opin. Anesthesiol. 18, 625–631. doi:10.1097/01.aco.0000189879.67092.12.

Huetz, C., Philibert, B., Edeline, J.M., 2009. A spike-timing code for discriminating conspecific vocalizations in the thalamocortical system of anesthetized and awake guinea pigs. J. Neurosci. 29, 334–350.
Ibañez, V., Deiber, M.P., Fischer, C., 1989. Middle latency auditory evoked potentials in cortical lesions. Critical of interhemispheric asymmetry. Arch. Neurol. 46, 1325–1332.
IMPReSS, 2022. ABR Protocol. International Mouse Phenotyping Resource of Standardised Screens.
Johnson, J.M., 2009. Late auditory event-related potentials in children with cochlear implants: a review. Dev. Neuropsychol. 34, 701–720. doi:10.1080/87565640903265152.
Joris, P.X., Schreiner, C.E., Rees, A., 2004. Neural processing of amplitude-modulated sounds. Physiol. Rev. 84, 541–577. doi:10.1152/physrev.00029.2003.
Knight, R.T., Brailowsky, S., Scabini, D., Simpson, G.V., 1985. Surface auditory evoked potentials in the unrestrained rat: component definition. Electroencephalogr. Clin. Neurophysiol. 61, 430–439. doi:10.1016/0013-4694(85)91035-1.
Land, R., Burghard, A., Kral, A., 2016. The contribution of inferior colliculus activity to the auditory brainstem response (ABR) in mice. Hear. Res. 341, 109–118. doi:10.1016/j.heares.2016.08.008.
Laumen, G., Ferber, A.T., Klump, G.M., Tollin, D.J., 2016. The physiological basis and clinical use of the binaural interaction component of the auditory brainstem response. Ear Hear. 37, e276–e290. doi:10.1097/AUD.0000000000000301.
Litscher, G., 1995. Middle latency auditory evoked potentials in intensive care patients and normal controls. Int. J. Neurosci. 83, 253–267. doi:10.3109/00207459508986342.
Madler, C., Keller, I., Schwender, D., Pöppel, E., 1991. Sensory information processing during general anaesthesia: effect of isoflurane on auditory evoked neuronal oscillations. Br. J. Anaesth. 66, 81–87. doi:10.1093/bja/66.1.81.
Manninen, P.H., Lam, A.M., Nicholas, J.F., 1985. The effects of isoflurane and isoflurane-nitrous oxide anesthesia on brainstem auditory evoked potentials in humans. Anesth. Analg. 64, 43–47.
McGee, T.J., Özdamar, Ö., Kraus, N., 1983. Auditory middle latency responses in the guinea pig. Am. J. Otolaryngol. 4, 116–122. doi:10.1016/S0196-0709(83)80013-1.
McPherson, D.L., Starr, A., 1993. Binaural interaction in auditory evoked potentials: brainstem, middle- and long-latency components. Hear. Res. 66, 91–98. doi:10.1016/0378-5955(93)90263-Z.
Metzger, K.L., Maxwell, C.R., Liang, Y., Siegel, S.J., 2007. Effects of nicotine vary across two auditory evoked potentials in the mouse. Biol. Psychiatry 61, 23–30. doi:10.1016/j.biopsych.2005.12.011.
Murofushi, T., Kaga, K., Asakage, T., 1994. Temporary latency shifts in auditory evoked potentials by injection of lidocaine in the rat. Hear. Res. 76, 53–59. doi:10.1016/0378-5955(94)90086-8.
Musiek, F., Nagle, S., 2018. The middle latency response: a review of findings in various central nervous system lesions. J. Am. Acad. Audiol. 29, 855–867. doi:10.3766/jaaa.16141.
Noda, T., Takahashi, H., 2015. Anesthetic effects of isoflurane on the tonotopic map and neuronal population activity in the rat auditory cortex. Eur. J. Neurosci. 42, 2298–2311. doi:10.1111/ejn.13007.
O'Reilly, J.A., Conway, B.A., 2021. Classical and controlled auditory mismatch responses to multiple physical deviances in anaesthetised and conscious mice. Europ. J. Neurosci. 53, 1839–1854. doi:10.1111/ejn.15072.
Özdamar, Ö., Kraus, N., Grossman, J., 1986. Binaural interaction in the auditory middle latency response of the guinea pig. Electroencephalogr. Clin. Neurophysiol. 63, 476–483. doi:10.1016/0013-4694(86)90129-X.
Picton, T.W., Hillyard, S.A., Krausz, H.I., Galambos, R., 1974. Human auditory evoked potentials. I: evaluation of components. Electroencephalogr. Clin. Neurophysiol. 36, 179–190. doi:10.1016/0013-4694(74)90155-2.
Raz, A., Grady, S.M., Krause, B.M., Uhlrich, D.J., Manning, K.A., Banks, M.I., 2014. Preferential effect of isoflurane on top-down vs. bottom-up pathways in sensory cortex. Front. Syst. Neurosci. 8, 191. doi:10.3389/fnsys.2014.00191.
Rosburg, T., Mager, R., 2021. The reduced auditory evoked potential component N1 after repeated stimulation: refractoriness hypothesis vs. habituation account. Hear. Res. 400, 108140. doi:10.1016/j.heares.2020.108140.
Ruebhausen, M.R., Brozoski, T.J., Bauer, C.A., 2012. A comparison of the effects of isoflurane and ketamine anesthesia on auditory brainstem response (ABR) thresholds in rats. Hear. Res. 287, 25–29. doi:10.1016/j.heares.2012.04.005.
Scimemi, P., Santarelli, R., Selmo, A., Mammano, F., 2014. Auditory brainstem responses to clicks and tone bursts in C57 BL/6 J mice. Acta Otorhinolaryngol. Ital. 34, 264–271.
Siegel, S.J., Connolly, P., Liang, Y., Lenox, R.H., Gur, R.E., Bilker, W.B., Kanes, S.J., Turetsky, B.I., 2003. Effects of Strain, Novelty, and NMDA blockade on auditory-evoked potentials in mice. Neuropsychopharmacology 28, 675–682. doi:10.1038/sj.npp.1300087.
Simosky, J.K., Stevens, K.E., Adler, L.E., Freedman, R., 2003. Clozapine improves deficient inhibitory auditory processing in DBA/2 mice, via a nicotinic cholinergic mechanism. Psychopharmacology (Berl.) 165, 386–396. doi:10.1007/s00213-002-1285-x.
Simpson, G.V., Knight, R.T., 1993. Multiple brain systems generating the rat auditory evoked potential. II. Dissociation of auditory cortex and non-lemniscal generator systems. Brain Res. 602, 251–263. doi:10.1016/0006-8993(93)90690-O.
Supp, G.G., Higgen, F.L., Hipp, J.F., Engel, A.K., Siegel, M., 2018. Mid-latency auditory evoked potentials differentially predict sedation and drug level under opioid and hypnotic agents. Front. Pharmacol. 9.
Tremblay, K.L., Burkard, R.F., 2012. Translational Perspectives in Auditory Neuroscience: Hearing Across the Life Span — Assessment and Disorders. Plural Publishing.
Winkler, I., Denham, S., Escera, C., 2013. Auditory Event-related Potentials. In: Jaeger, D., Jung, R. (Eds.), Encyclopedia of Computational Neuroscience. Springer, New York, New York, NY, pp. 1–29. doi:10.1007/978-1-4614-7320-6_99-1.
Woods, D.L., Clayworth, C.C., Knight, R.T., Simpson, G.V., Naeser, M.A., 1987. Generators of middle- and long-latency auditory evoked potentials: implications from studies of patients with bitemporal lesions. Electroencephalogr. Clin. Neurophysiol./Evoked Potentials Section 68, 132–148. doi:10.1016/0168-5597(87)90040-2.
Yang, J.-.W., An, S., Sun, J.-J., Reyes-Puerta, V., Kindler, J., Berger, T., Kilb, W., Luhmann, H.J., 2013. Thalamic network oscillations synchronize ontogenetic columns in the newborn rat barrel cortex. Cerebral Cortex 23, 1299–1316. doi:10.1093/cercor/bhs103.
Zhang, Q., Liu, H., McGee, J., Walsh, E.J., Soukup, G.A., He, D.Z.Z., 2013. Identifying MicroRNAs involved in degeneration of the organ of corti during age-related hearing loss. PLoS ONE 8, e62786. doi:10.1371/journal.pone.0062786.
Zinnamon, F.A., Harrison, F.G., Wenas, S.S., Meyer, A.F., Liu, Q., Wang, K.H., Linden, J.F., 2019. Hearing loss promotes schizophrenia-relevant brain and behavioral abnormalities in a mouse model of human 22q11.2 deletion syndrome. bioRxiv 539650. doi:10.1101/539650.